

Electron transport in a two-dimensional electron gas with magnetic barriers

T. Vančura, T. Ihn, S. Broderick, and K. Ensslin

Laboratory of Solid State Physics, ETH Zürich, 8093 Zürich, Switzerland

W. Wegscheider^{1,2} and M. Bichler¹

¹*Walter-Schottky Institut, Technische Universität München, 85748 Garching, Germany*

²*Institut für Angewandte und Experimentelle Physik, Universität Regensburg, 93040 Regensburg, Germany*

(Received 29 November 1999)

The low-temperature longitudinal and Hall resistances of a two-dimensional electron gas are studied in the presence of a magnetic barrier created under the edge of a thin ferromagnetic film. An in-plane external magnetic field allows us to tune the barrier height within the classically transmissive regime. A theoretical model is presented that predicts the size and shape of the resistance correction for the ballistic case in the presence of a single magnetic barrier. The model that contains no adjustable parameters is in qualitative agreement with the experiment. The size of the predicted resistance correction agrees with the measurement within a factor of 2.

Electrical transport of electrons in two dimensions in the presence of inhomogeneous magnetic fields raises fundamental questions and promises the realization of novel devices. Experiments focusing on fundamental issues used random inhomogeneous magnetic fields created either by vortices in superconductors¹ or by ferromagnetic layers² placed on top of a two-dimensional electron gas (2DEG). Electron transport involving periodic magnetic field modulation was also studied experimentally.^{3,4} While the first of these experiments were devoted to the observation of commensurability effects,³ a novel giant classical magnetoresistance due to the presence of the periodic arrangement of magnetic barriers was discovered.⁴

In recent experiments the number of magnetic barriers has been decreased down to the least involved case of a single barrier.^{5–8} In Ref. 5 a 3 μm thick magnetic barrier could be realized in a nonplanar 2DEG. In other studies^{6–8} a different approach was used: if a thin magnetic film is placed on top of a heterostructure its in-plane magnetization can be saturated in an external in-plane magnetic field. In this case the out-of-plane component of the fringe field under the edge of the film creates a magnetic barrier for electron transport with a width of the order of 100 nm determined by the separation of the 2DEG from the magnetic film. Magnetic field strengths of more than 0.5 T have been realized.⁸ In Ref. 7 the utilization of such an arrangement as a ‘‘hybrid Hall effect device’’ was suggested. The theory and modeling relevant for these experiments is due to Peeters and co-workers.^{9–14} They concentrated on the Hall resistance in the ballistic¹² and in the diffusive regime^{13,14} and presented results for the longitudinal resistance in the diffusive regime.¹³

In this paper we present low-temperature measurements of the longitudinal and Hall resistances in ferromagnetic/semiconductor hybrid devices of the same type used by Kubrak *et al.* in Ref. 8. Our results for the longitudinal resistance in the presence of magnetic barriers in the classically transmissive regime are qualitatively similar to those reported by these authors for magnetic barriers saturating in

the classically opaque regime. We propose a transport model for the longitudinal resistance in the presence of a magnetic barrier for the ballistic regime and compare it with the experimental findings. It is found that the model predicts a V-shaped resistance correction in qualitative agreement with the experiments. The size of the resistance correction agrees within a factor of 2 with the experiment. We find experimentally that in addition to the magnetic barrier, fringe fields are present in the electron gas during magnetization reversal of the film, which may diminish the resistance correction observed in our experiment.

The samples investigated in this study are based on a conventional GaAs/Al_{0.3}Ga_{0.7}As heterostructure grown by molecular beam epitaxy with the heterointerface 37 nm below the sample surface. Hall bar structures were fabricated with photolithographic techniques as depicted schematically in Fig. 1(a). The width of the Hall bar is $W = 20 \mu\text{m}$, the

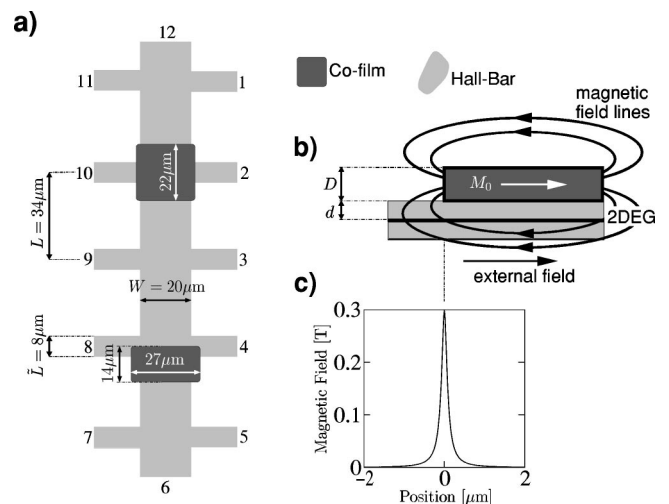


FIG. 1. (a) Schematic sample overview. (b) Schematic cross section through the sample with the cobalt film placed above the 2DEG. (c) Magnetic field profile of the magnetic barrier created in the electron gas under the edge of the film.

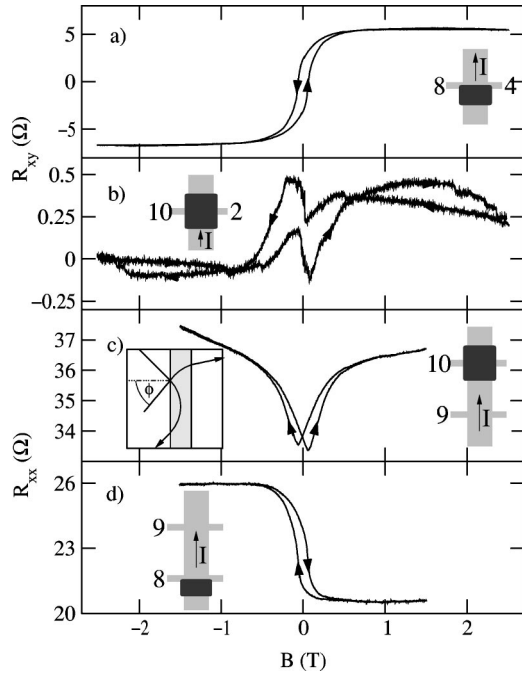


FIG. 2. (a)–(d) Measurements of R_{xx} and R_{xy} vs parallel magnetic field using different contact pairs as indicated by the schematic insets. Left inset in (c): typical classical electron trajectories (one transmitted, the other reflected).

separation of neighboring voltage probes is $L = 34 \mu\text{m}$, and the width of each voltage probe is $\bar{L} = 8 \mu\text{m}$. Two rectangular films of cobalt with a thickness of 100 nm and covered with 30 nm of gold were deposited at a pressure of about 10^{-6} mbar on top of the Hall bar structure as shown in Figs. 1(a) and 1(b). Their dimensions are $22 \mu\text{m} \times 22 \mu\text{m}$ and $27 \mu\text{m} \times 14 \mu\text{m}$, respectively.

All measurements shown below were carried out in a ^4He cryostat at temperatures down to 1.7 K. They were recorded using the standard lock-in technique with a 73 Hz ac current between 100 nA and $5 \mu\text{A}$ applied between contacts 6 and 12 (see Fig. 1). A magnetic field was applied in the plane of the 2DEG (with an accuracy of $\pm 0.01^\circ$) and parallel to the direction of current flow. In order to avoid a hysteresis due to lock-in time constants, the magnet was not swept continuously but rather the field was set to a fixed value and after a time considerably longer than the lock-in time constant, the data point was taken. This corresponded to a sweep rate lower than 50 mT/min.

The electron sheet density was determined from classical Hall measurements and from the Shubnikov–de Haas effect to be $n = 5.5 \times 10^{15} \text{ m}^{-2}$. The Hall mobility is $\mu = 70 \text{ m}^2/\text{Vs}$ at 1.7 K, giving an elastic mean free path of $l_{el} = 8.6 \mu\text{m}$.

In Fig. 2(a) we show the Hall resistance R_{xy} measured between voltage probes 4 and 8. It shows the hysteresis of the cobalt film that is reflected in the normal component of the fringe field penetrating the active area of the Hall cross. From this measurement we determine the saturation value $\Delta R_{xy} = 6.25 \Omega$ and a coercive field of $B_c = 60 \text{ mT}$. The curve apparently shows the symmetry $R_{xy}^{(\text{sweep up})}(B) = -R_{xy}^{(\text{sweep down})}(-B)$ expected from the corresponding symmetry of the magnetization of the cobalt film. The measure-

ment is consistent with the idea that the magnetic fringe field of the cobalt film creates a magnetic barrier in the electron gas right under the edge of the film [see Fig. 1(b,c)]. This inhomogeneous field distribution in the Hall cross causes the measured Hall signal.

Figure 2(b) shows R_{xy} measured between voltage probes 2 and 10, i.e., under the center of the square cobalt film. Note that the resistance scale differs by a factor of 20 compared to Fig. 2(a). Again a hysteresis with a similar symmetry is observed, but it differs in magnitude and in the characteristic field scale from that in Fig. 2(a). The main hysteretic feature appears below a field of $|B| < 1 \text{ T}$. But even up to fields of $|B| = 2.5 \text{ T}$ down and up sweeps give different R_{xy} and, unlike in the case of Fig. 2(a), $R_{xy}^{(\text{sweep up})} > R_{xy}^{(\text{sweep down})}$ is observed. This hysteresis sits on top of a step of the Hall signal of magnitude $2\Delta R_{xy} = 0.35 \Omega$. This step is most likely due to an asymmetric placement of the square cobalt film with respect to the voltage probes in the direction of the current. This measurement shows that even below the cobalt film there exist fringe fields that mainly come into play during the process of magnetization reversal. These fringe fields are (almost) absent at large external magnetic fields and also around zero external field.

In Fig. 2(c) the longitudinal resistance R_{xx} measured between voltage probes 9 and 10 is shown. A V-shaped hysteretic dip with a magnitude of about 3Ω is observed in the region where R_{xy} in Fig. 2(a) is hysteretic as well. These curves are qualitatively similar to those reported in Ref. 8. In our measurement the cusps occur at the coercive field $B_c = \pm 60 \text{ mT}$ and the curves have the dominant symmetry $R_{xx}^{(\text{sweep up})}(B) = R_{xx}^{(\text{sweep down})}(-B)$. Choosing different pairs of voltage probes for measurements of $R_{xx}(B)$ allows us to measure pieces of the Hall bar with up to four magnetic barriers in series. We find that the magnitude of the dips $\Delta R_{xx} = R_{xx}(B = 1.5 \text{ T}) - R_{xx}(B_c)$ is a linear function of the number of magnetic barriers with a slope of 3.5Ω per barrier. We find a relative deviation of not more than $\pm 3.5\%$ from this value for any individual barrier.

In Fig. 2(d) we show the longitudinal resistance measured between the voltage probes 8 and 9. The hysteresis curve shows neither the symmetry of R_{xx} nor that of R_{xy} but rather seems to contain both contributions. This behavior is expected in the diffusive as well as in the ballistic regime. In the former, the presence of the magnetic barrier leads to a finite Hall angle in the Hall cross between contacts 8 and 4. A part of the corresponding Hall voltage will appear on the potential of contact 8 and therefore appears in the longitudinal resistance measured between 8 and 9. In the ballistic case the magnetic barrier affects the symmetry of the transmission coefficients between the contacts under consideration, leading to an antisymmetric contribution to the longitudinal resistance as well. From these arguments it is plausible that this is also the case for the intermediate range between the ballistic and the diffusive transport regime.

In accordance with Ref. 14 we calculate the magnetic field profile in the 2DEG resulting at the edge of the cobalt film due to its magnetization. Under the assumption that the width of the cobalt film exceeds the width of the Hall bar (in our case by several hundred nanometers) we arrive at the expression

$$B_z(x) = \frac{\mu_0 M_s}{4\pi} \ln \frac{x^2 + d^2}{x^2 + (d+D)^2} \quad (1)$$

for the field component normal to the electron gas, where M_s is the saturation magnetization of cobalt, x is measured along the Hall bar with $x=0$ under the edge of the film, D is the film thickness, and d is the distance from the 2DEG to the cobalt film. Using this formula with the saturation magnetization for bulk cobalt of $\mu_0 M_s = 1.8$ T and the geometric dimensions of our samples, we arrive at the magnetic field profile depicted in Fig. 1(c). It should be emphasized at this point that the process of magnetization reversal in thin films is complicated and hard to predict theoretically. Equation (1) should be valid at high magnetic fields where the magnetization of the cobalt film can be assumed to be saturated in the direction of the external field. Lowering the magnetic field will in general not only lead to a steady decrease of the magnitude of the magnetization M from its saturation value M_s , but at the same time domain walls will be formed. It is evident from Fig. 2(b) that additional fringe fields are present in the 2DEG at external fields $|B| < 0.5$ T. In Ref. 7 it was shown that in a square film in the absence of any external magnetic field four domains appear whose magnetization vectors form a closed loop. Such a configuration would not lead to fringe fields in the electron gas.

The results of model calculations^{12,13,15,16} suggest that the Hall resistance in the presence of inhomogeneous magnetic fields takes the general form

$$R_{xy} = \frac{\alpha^* \langle B_z \rangle}{ne}, \quad (2)$$

where $\langle B_z \rangle$ is the normal component of the magnetic field averaged over the area of the Hall cross and α^* is a constant which depends on the geometry of the structure and on the elastic mean free path. In the case of a ballistic Hall cross $\alpha^* = 1$ has been shown.¹² In the diffusive case the active area can be larger since the diffusing electron can probe the magnetic field a certain distance away from the Hall cross and still diffuse back into one of the Hall contacts.^{13,15,16} This leads to values $\alpha^* < 1$.¹³ This approach involving the average magnetic field is assumed to suffice here, though it may not properly account for drifting states due to the van Alphen drift.

The average magnetic field in the Hall cross is $\langle B_z \rangle = cM_s/\tilde{L}$. The constant c has the dimension of a length and can be obtained from Eq. (1) by integrating the logarithmic term over the extent of the barrier. It depends on d and D and is in our case given by $c = 49$ nm (calculated with $D = 100$ nm, $d = 42$ nm, i.e., 37 nm cap plus 5 nm average wavefunction setback). The measured Hall signal at large external magnetic fields is $R_{xy} = 6.25 \Omega$ [see Fig. 2(a)]. Assuming that the magnetization of the cobalt film is saturated at its literature value of $\mu_0 M_s = 1.8$ T we determine $\alpha^* = 0.50$. This value seems to be rather low for a system in which l_{el} is comparable to \tilde{L} . An alternative interpretation would assume $\alpha^* = 1$ as expected for ballistic systems and conclude that the magnetic barrier height corresponds to an effective magnetization of the cobalt film, which is about half the literature value. Although the latter interpretation seems to be unlikely,

since excellent agreement with the literature value for the saturation was achieved, e.g., in Ref. 17, we will pursue these two extreme variants ($\alpha^* = 0.5, 1$) in the following and work out their consequences.

For the discussion of the longitudinal resistance R_{xx} in Fig. 2(c), i.e., the electron transport across the magnetic barrier, we introduce the critical angle (following Ref. 8) $\phi_c = \arcsin[1 - (ecM_s)/(\hbar k_F)]$. The angle ϕ is measured between the axis along the Hall bar (x axis) and the direction of the velocity vector of an electron incident on the barrier [see inset of Fig. 2(c)]. The angle dependent transmission $T(\phi)$ for an electron is $T(\phi) = 0$ if $\phi_c < \phi < \pi/2$ and $T(\phi) = 1$ otherwise. Following the semiclassical approach in Ref. 18 we calculate the average classical transmission through the barrier

$$\langle T \rangle = \frac{1}{2} \int_{-\pi/2}^{+\pi/2} \cos \phi T(\phi) d\phi = 1 - \frac{ecM_s}{2\hbar k_F}. \quad (3)$$

With the literature value for the cobalt magnetization we compute for our arrangement $\langle T \rangle = 64\%$. If the effective barrier height is only half its expected value we have $\langle T \rangle = 82\%$. A full quantum-mechanical description of the transmission can be found in Ref. 9.

The contribution of the magnetic barrier acting as an additional scatterer to the longitudinal resistance can be estimated following the Landauer formula

$$\Delta R = \frac{h}{2e^2 N} \frac{1 - \langle T \rangle}{\langle T \rangle}. \quad (4)$$

Here $N = 2W/\lambda_F$ is the number of modes across the Hall bar and λ_F is the Fermi wavelength of the electrons. With the above values $\langle T \rangle = 64\%$ and $\langle T \rangle = 82\%$ the corrections are expected to be $\Delta R = 6.1 \Omega$ and $\Delta R = 2.4 \Omega$, respectively. As mentioned above we determine $\Delta R = 3.5 \Omega$ for a single barrier in the experiment, which is well within the prediction of the model. The model assumes that the transport across the magnetic barrier is phase coherent and ballistic. In view of a barrier width of about 100 nm compared to a mean free path of more than 8 μm the latter assumption seems to be a good first approximation. In measurements of the temperature dependence of the resistance only little changes are observed in ΔR up to 77 K, indicating that neither quantum effects nor phase coherence play a significant role here. Nevertheless we state that according to the theory¹⁹ we expect a phase coherence length of more than 30 μm at 1.7 K in our structures.

It is tempting to use a magnetic-field-dependent magnetization $M(B)$ in Eq. (3) instead of M_s , which leads to a magnetic-field-dependent average transmission $\langle T(B) \rangle$. This allows to predict a magnetic-field-dependent $\Delta R(B)$ from Eq. (4). $M(B)$ can be extracted from the measurement of $R_{xy}(B)$ in Fig. 2(a) using Eq. (2), since $\langle B_z \rangle = cM(B)/\tilde{L}$. The result of such a procedure is depicted in Fig. 3(a) (dotted lines). It is characteristic for this model that around the coercive field $\Delta R(B)$ increases linearly with the external magnetic field, which is due to the fact that the Hall resistance can be approximated by a linear function around B_c . At large fields $\Delta R(B)$ saturates due to the saturation of the magnetization $M(B)$. We emphasize that this model contains no free parameters and makes a prediction for the size of the

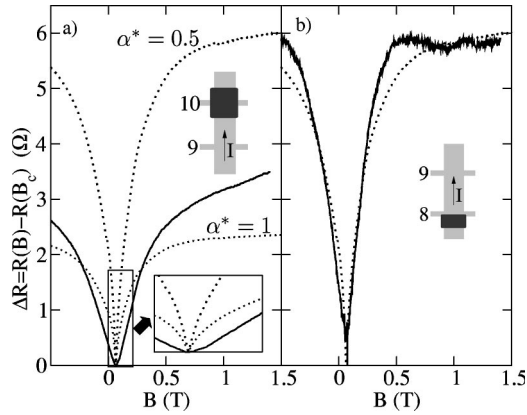


FIG. 3. (a) Dotted lines: Predicted behavior of ΔR according to the model described in the text corresponding to different values for α^* . Solid line: $\Delta R(B)$ measured between probes 9 and 10. (b) Dotted line: Predicted behavior of ΔR . Solid line: $\Delta R(B)$ obtained from the symmetric contribution to the measurement between probes 8 and 9 (scaled by a factor of 6.2).

resistance correction. The shape of $\Delta R(B)$ may be inferred from the shape of the hysteresis in R_{xy} .

For comparing the measured $\Delta R(B)$ [Fig. 2(c)] with the predictions of the model for the two cases ($\alpha^*=0.5,1$) we show measurement and model in Fig. 3(a). Although the measured size of the effect is well described by the model, the actual shape of the measured curve differs from the model. Especially around B_c the sharp linear increase of ΔR in the model is not observed in the measurement. The same observation has also been made by Kubrak *et al.* in their structures.^{8,20} In addition, one observes in Fig. 3(a) that the curvature of the measured curve has the opposite sign of that of the predicted curves.

We suggest that the assumption that only the magnetic barrier at the edge of the cobalt film determines $\Delta R(B)$ may not be justified for this measurement. If we measure R_{xx} between voltage probes 9 and 10 we are sensitive to any fringe fields in the whole area between these two contacts [see inset of Fig. 3(a)]. Since during magnetization reversal in addition to the magnetic barrier at the film edge fringe fields arise *under* the film [as is evident from Fig. 2(b)], $\Delta R(B)$ will be raised by these additional field inhomogeneities, especially in the region of $|B| < 1$ T. This influence diminishes the magnitude of the observable resistance correction ΔR and modifies the detailed shape of the $\Delta R(B)$ curves.

In order to support this hypothesis experimentally we compare the symmetrized resistance measured between voltage probes 8 and 9 with the predicted curve for $\alpha^*=0.5$ in Fig. 3(b). It is necessary to symmetrize the data according to $R_{\text{symm}}^{(\text{sweep up})}(B) = [R_{xx}^{(\text{sweep up})}(B) + R_{xx}^{(\text{sweep down})}(-B)]/2$ since

the voltage in probe 8 contains a significant contribution from the Hall effect. The difference between the measurement between contacts 9 and 10 and that between 8 and 9 lies in the fact that the former (9-10) probes a certain region under the cobalt film while the latter (8-9) is sensitive only to the region under the edge of the film. However, since probe 8 averages over the potential on both sides of the magnetic barrier the measured ΔR will be smaller than that measured between 9 and 10. The symmetrized $\Delta R(B)$ values are therefore multiplied by a factor of 6.2 to the size of 6 Ω and plotted in Fig. 3(b) (solid line) together with the model (dotted line). The measured curve does indeed produce the expected shape around B_c and even reproduces the expected slope $d[\Delta R(B)]/dB$. A similar multiplication with the experimental curve in Fig. 3(a) does not at all agree with the prediction. These results support the hypothesis that $\Delta R(B)$ measured between contacts 9 and 10 is influenced by inhomogeneous stray fields under the cobalt film occurring during magnetization reversal.

Our model is based on various assumptions that we wish to highlight. First, we have assumed that $M(B) \propto R_{xy}(B)$, which implies that α^* is independent of B and results in $\Delta R \propto |B - B_c|$ in the limit $B \rightarrow B_c$. Second, we assume ideal barriers and do not take any fluctuations in the barrier height or in the barrier position into account that may arise due to imperfections of the magnetic film. Third, we neglect elastic scattering events that may occur during an electron traverse of the barrier. Further experimental and theoretical efforts are necessary in order to clarify the detailed shape of the measured V-shaped resistance.

In conclusion, we have studied the electron transport across single magnetic barriers in a 2DEG created by the deposition of a thin ferromagnetic cobalt film with the emphasis on understanding the correction of the longitudinal resistance. To this end we have presented a model suitable for the ballistic transport across the barrier, which predicts the size and the shape of the resistance correction $\Delta R(B)$ from the knowledge of the barrier height at different external magnetic fields. The accurate determination of the latter with electrical transport experiments has not yet been achieved. Taking this uncertainty into account the measured size of the resistance correction is well predicted by the model. We suggest that the resistance correction deviates from the prediction of the model if the area between the voltage pairs covers a significant region under the magnetic film. Fringe fields occurring under the film during magnetization reversal may contribute to this deviation.

We gratefully acknowledge fruitful discussions with F. M. Peeters, B. L. Gallagher, V. Kubrak, and C. Back and the help of S. Lindemann during sample preparation. This project was financially supported through the ETH Zurich.

¹S. J. Bending, K. von Klitzing, and K. Ploog, Phys. Rev. Lett. **65**, 1060 (1990); A. K. Geim, S. J. Bending, and I. V. Grigorieva, *ibid.* **69**, 2252 (1992); A. K. Geim, S. J. Bending, I. V. Grigorieva, and M. G. Blamire, Phys. Rev. B **49**, 5749 (1994); A. Smith, R. Taboryski, L. T. Hansen, C. B. Sorensen, P. Hede-

gard, and P. E. Lindelof, *ibid.* **50**, 14 726 (1994).

²F. B. Mancoff, R. M. Clarke, C. M. Marcus, S. C. Zhang, K. Campman, and A. C. Gossard, Phys. Rev. B **51**, 13 269 (1995); F. B. Mancoff, L. J. Zielinski, C. M. Marcus, K. Campman, and A. C. Gossard, *ibid.* **53**, R7599 (1996); A. W. Rushforth, B. L.

- Gallagher, P. C. Main, A. C. Neumann, C. H. Marrows, I. Zoller, M. A. Howson, B. J. Hickey, and M. Henini, *Physica E* **6**, 751 (2000).
- ³H. A. Carmona, A. K. Geim, A. Nogaret, P. C. Main, T. J. Foster, M. Henini, S. P. Beaumont, and M. G. Blamire, *Phys. Rev. Lett.* **74**, 3009 (1995); P. D. Ye, D. Weiss, R. R. Gerhardts, M. See-ger, K. von Klitzing, K. Eberl, and H. Nickel, *ibid.* **74**, 3013 (1995); P. D. Ye, D. Weiss, K. von Klitzing, K. Eberl, and H. Nickel, *Appl. Phys. Lett.* **67**, 1441 (1995); H. A. Carmona, A. Nogaret, A. K. Geim, P. C. Main, T. J. Foster, M. Henini, S. P. Beaumont, H. McLelland, and M. G. Blamire, *Surf. Sci.* **361/362**, 328 (1996).
- ⁴A. Nogaret, S. Carlton, B. L. Gallagher, P. C. Main, M. Henini, R. Wirtz, R. Newbury, M. A. Howson, and S. P. Beaumont, *Phys. Rev. B* **55**, R16 037 (1997); N. Overend, A. Nogaret, B. L. Gallagher, P. C. Main, M. Henini, C. H. Marrows, M. A. Howson, and S. P. Beaumont, *Appl. Phys. Lett.* **72**, 1724 (1998); N. Overend, A. Nogaret, B. L. Gallagher, P. C. Main, R. Wirtz, R. Newbury, M. A. Howson, and S. P. Beaumont, *Physica B* **249-251**, 326 (1998).
- ⁵M. L. Leadbeater, C. L. Foden, J. H. Burroughes, M. Pepper, T. M. Burke, L. L. Wang, M. P. Grimshaw, and D. A. Ritchie, *Phys. Rev. B* **52**, R8629 (1995).
- ⁶F. G. Monzon, M. Johnson, and M. L. Roukes, *Appl. Phys. Lett.* **71**, 3087 (1997).
- ⁷M. Johnson, B. R. Bennet, M. J. Yang, M. M. Miller, and B. V. Shangbrook, *Appl. Phys. Lett.* **71**, 974 (1997).
- ⁸V. Kubrak, A. C. Neumann, B. L. Gallagher, P. C. Main, M. Henini, C. H. Marrows, and M. A. Howson, *Physica E* **6**, 755 (2000).
- ⁹F. M. Peeters and A. Matulis, *Phys. Rev. B* **48**, 15 166 (1993).
- ¹⁰A. Matulis, F. M. Peeters, and P. Vasilopoulos, *Phys. Rev. Lett.* **72**, 1518 (1994).
- ¹¹I. S. Ibrahim, V. A. Schweigert, and F. M. Peeters, *Phys. Rev. B* **56**, 7508 (1997).
- ¹²F. M. Peeters and X. Q. Li, *Appl. Phys. Lett.* **72**, 572 (1998).
- ¹³I. S. Ibrahim, V. A. Schweigert, and F. M. Peeters, *Phys. Rev. B* **57**, 15 416 (1998).
- ¹⁴J. Reijniers and F. M. Peeters, *Appl. Phys. Lett.* **73**, 357 (1998).
- ¹⁵S. J. Bending and A. Oral, *J. Appl. Phys.* **81**, 3721 (1997).
- ¹⁶S. Liu, H. Guillou, A. D. Kent, G. W. Stupian, and M. S. Leung, *J. Appl. Phys.* **83**, 6161 (1998).
- ¹⁷M. Kato, A. Endo, S. Katsumoto, and Y. Iye, *Phys. Rev. B* **58**, 4876 (1998).
- ¹⁸C. W. J. Beenakker and H. van Houten, *Phys. Rev. Lett.* **63**, 1857 (1989).
- ¹⁹B. L. Altshuler and A. G. Aronov, in *Electron-Electron Interactions in Disordered Systems*, edited by A. L. Efros and M. Pollak (Elsevier Science, Amsterdam, 1985), p. 1.
- ²⁰V. Kubrak, B. Gallagher, and P. Main (private communication).